

## A SIMPLE AND HIGHLY EFFICIENT METHOD FOR THE SYNTHESIS OF KNOEVENAGEL CONDENSATION PRODUCTS BY USING Cu–Cu<sub>2</sub>O–SiO<sub>2</sub> NANOCOMPOSITE



**R. K. Dhokale**

Department of Chemistry, Arts, Science and Commerce College,  
Naldurg, Dist. Osmanabad (MS), INDIA.  
Corresponding author: rkdhokale@gmail.com

### Authors Short Profile

R. K. Dhokale is working at Department of Chemistry in Arts, Science and Commerce College, Naldurg, Dist. Osmanabad (MS), INDIA.

### Abstract :

The condensation reaction has been carried out very conveniently to obtain the corresponding Knoevenagel condensation products in excellent yields. The reaction conditions are very mild and applicable to 4-Bromobenzaldehyde with different active methylene compounds.

### KEYWORDS :

Methylene compounds, organic chemistry.

### 1 INTRODUCTION

In past decades, several carbon-carbon bond-forming reactions have been discovered, and their applications in organic chemistry have also been well documented in the literature [1–6]. Base-catalyzed transformations are frequently used both on small scale as well as large scale in organic synthesis, for example, in Aldol [7], Knoevenagel [8], Henry [9], and Michael [10] reactions. To catalyze these processes, organic amines, alkali alkoxides, and alkali hydroxides are commonly used as a homogeneous phase with the reagents. Although effective, these reagents are difficult to separate and, in many cases, are not recycled. To alleviate this problem, solid basic catalysts have been developed utilizing either inorganic solid materials, such as base metal oxides and carbonates, or by supporting organic bases, for example, amines, on inorganic or polymeric supports. This approach has attracted intense interest and has been reviewed extensively [11, 12]. Effective heterogeneous base catalysis have been found for Aldol [13–15], Knoevenagel [16–18], Henry [19, 20], and Michael [21] reactions, and, in many, cases the solid base is recyclable [22].

In this communication we report the scope use of Cu–Cu<sub>2</sub>O–SiO<sub>2</sub> for Knoevenagel condensation, which proved to be excellent. It is observed that a combination of Cu–Cu<sub>2</sub>O–SiO<sub>2</sub> shows enhanced catalytic activity due to well dispersion of catalytic centres. With this aim, a series of Cu–Cu<sub>2</sub>O–SiO<sub>2</sub>

nanocomposites, having different concentrations of copper, has been synthesized and studied its catalytic activity for the Knoevenagel condensation at room temperature.

## 2 EXPERIMENTAL DETAILS

All chemicals used were of AR grade. For the synthesis of Cu-Cu<sub>2</sub>O-SiO<sub>2</sub> nanocomposites, the different chemical such as copper acetate, sodium dodecyl sulphate as a capping agents, hydrazine hydrate as a reducing agent, commercial silica were used. The 4-Bromobenzaldehyde and different active methylene compounds were used for Knoevenagel condensation.

### 2.1 Preparation of Cu-Cu<sub>2</sub>O-SiO<sub>2</sub> nanocomposites.

Cu-Cu<sub>2</sub>O-SiO<sub>2</sub> nanocomposites were synthesized by chemical reduction followed by impregnation method. The copper nanoparticles were synthesised by using chemical reduction method. 5 mL (1x10<sup>-2</sup> M) copper acetate solution and 5 mL (1x10<sup>-2</sup> M) sodium dodecyl sulphate were mixed together. The mixture was stirred at 60 °C for 30 min. 3 mL hydrazine hydrate solution was added drop by drop with constant stirring in oil bath keeping the temperature at 60 °C. The dark coloured slurry/residue was obtained. The content was centrifuged, washed with distilled water, ethanol and dried.

For making composite, the copper nanoparticles were dispersed into 100 mg silica powder with 5 mL distilled water. The resulting mixture was stirred for 2-3 hours at room temperature. In the nanocomposites, the amount of copper was varied from 5 wt %, 25 wt % and 50 wt%. The obtained residue was centrifuged, washed with water and dried. The product was used as a catalyst for Knoevenagel condensation.

### 2.2 Characterization of Cu-Cu<sub>2</sub>O-SiO<sub>2</sub> nanocomposites

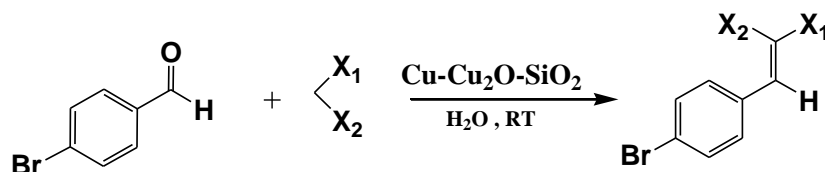
X-ray diffractometer (Philips model PW-1710) was used to identify the structural properties of the samples using Cu K $\alpha$  radiation. Energy-dispersive spectroscopy technique (JSM-JEOL 6360) was used for the elemental analysis of the Cu-Cu<sub>2</sub>O-SiO<sub>2</sub> nanocomposites. Particle morphology was measured using a transmission electron microscope (TEM) (Philips, CM200, operating voltages 20–200 kV). The UV-visible (UV-visible) spectra of the powders were recorded using a (JASCO model V-670) spectrophotometer equipped with an integrating sphere accessory. Barium sulphate was used as reference for the reflectance spectra. Fourier transform Infra-red (FT-IR) spectra of the catalysts were recorded in a Perkin-Elmer spectrometer using KBr pellets. The photoluminescence (PL) measurements of the samples were carried out by using Spectrofluorimeter (JASCO FP-750).

### 2.3 Catalytic activity

The catalytic properties of Cu-Cu<sub>2</sub>O-SiO<sub>2</sub> system were examined by Knoevenagel condensation. This condensation was conducted between 4-Bromobenzaldehyde and different active methylene compounds in water as a solvent. In this reaction, the mixture of 4-Bromobenzaldehyde (1 mmol), malononitrile (1 mmol), Cu-Cu<sub>2</sub>O-SiO<sub>2</sub> (10 mg) catalyst with distilled water was taken in RB flask and stirred continuously at room temperature. The progress of the reaction was monitored by TLC. After completion of reaction, the reaction mixture was treated with ethanol for separating the desired product and catalyst by filtration. The products were recrystallized by ethanol and thereafter the various experimental parameters such as melting points, reaction-time and yield of the products were noted. NMR spectra were taken in CDCl<sub>3</sub> using a Bruker Spectrospin Avance II-300MHz spectrophotometer and Jeol-400MHz spectrophotometer with TMS as an internal standard. The catalyst exhibited a clean reaction profile with excellent yields in a short reaction time. The

experimental data of all the products were consistent with the proposed structure. Same procedure was adopted for different active methylene compounds.

The general route for Cu-Cu<sub>2</sub>O-SiO<sub>2</sub> catalysed Knoevenagel condensation is given below:



### 3. RESULTS AND DISCUSSION

#### 3.1 X-ray diffraction studies

Fig. 1.1 shows the powder X-ray diffraction patterns of Cu-Cu<sub>2</sub>O and Cu-Cu<sub>2</sub>O-SiO<sub>2</sub> nanocomposites. All samples show peaks corresponding to well crystallized phase of metallic copper particles [JCPDS card no. 85-1326, 04-0836, 70-3038, 89-2883] with the presence of small intensity peaks for Cu<sub>2</sub>O particles [JCPDS No. 78-2076, 05-0667]. This observation reveals the presence of copper particles with Cu<sub>2</sub>O particles due to partial oxidation of surface copper particles [23]. The diffraction peaks with strong intensities appear at  $\sim 43.41^\circ$ ,  $\sim 50.36^\circ$ ,  $\sim 74.16^\circ$  are corresponds to (111), (200) and (220) planes of copper particles, respectively. These diffraction peaks corresponds to face-centered cubic structure of elemental copper with the space group of Fm3m [JCPDS No. 85-1326]. The diffraction peaks at  $\sim 36.27^\circ$  and  $\sim 61.34^\circ$  indicates the presence of Cu<sub>2</sub>O, which corresponds to the (110) and (211) plane. In the composites, the broad and diffuse diffraction peak of SiO<sub>2</sub> is observed at  $\sim 21.44^\circ$ , which is attributed to amorphous silica [24]. The crystallite size of copper as well as Cu<sub>2</sub>O NPs was calculated by using Scherrer's equation.

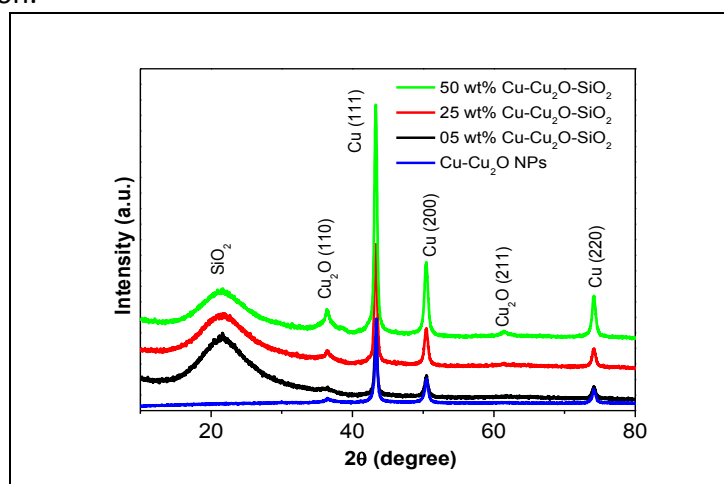


Fig. 1.1: Powder XRD patterns of (a) Cu-Cu<sub>2</sub>O nanoparticles, (b) Cu-Cu<sub>2</sub>O-SiO<sub>2</sub> (5 wt%), (c) Cu-Cu<sub>2</sub>O-SiO<sub>2</sub> (25 wt %). and (d) Cu-Cu<sub>2</sub>O-SiO<sub>2</sub> (50 wt %)

#### 3.2 TEM and EDAX studies

Fig. 1.2 (a–b) depicts the transmission electron micrographs of Cu-Cu<sub>2</sub>O and Cu-Cu<sub>2</sub>O-SiO<sub>2</sub> samples. It is evident from Fig. 1.2(a) that the average particle size of copper nanoparticles is found in the range of 10-15 nm. Fig. 1.2(b) clearly shows the presence of a dispersed phase of Cu-Cu<sub>2</sub>O particles

in the matrix of SiO<sub>2</sub>. The compositions of 5 wt% Cu-Cu<sub>2</sub>O-SiO<sub>2</sub>, 25 wt% Cu-Cu<sub>2</sub>O-SiO<sub>2</sub> and 50 wt% Cu-Cu<sub>2</sub>O-SiO<sub>2</sub> samples were determined by using the energy dispersive X-ray analysis (EDAX). Typical EDAX spectrum of 50 wt% Cu-Cu<sub>2</sub>O-SiO<sub>2</sub> sample is shown in Fig.1.3. The quantitative analysis of the EDAX spectrum revealed that the relative atomic ratios of Cu and Cu: Si are close to the initial values taken for three nanocomposites samples.

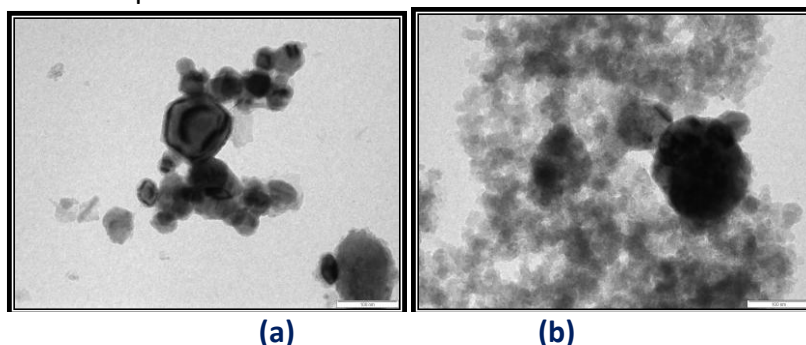


Fig. 1.2: TEM micrographs of (a) Cu-Cu<sub>2</sub>O, (b) Cu-Cu<sub>2</sub>O-SiO<sub>2</sub> (50 wt%).

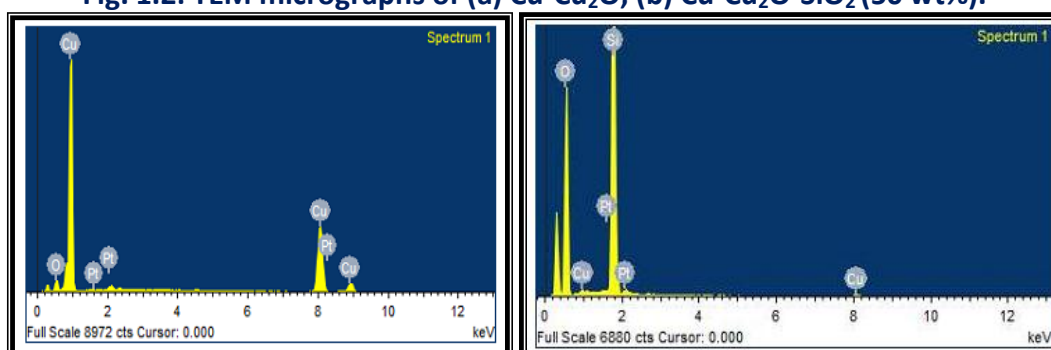


Fig. 1.3: EDAX patterns (a) Cu-Cu<sub>2</sub>O nanoparticles and (b) Cu-Cu<sub>2</sub>O-SiO<sub>2</sub> (50 wt %).

### 6.3.3 Photoluminescence measurements

The room temperature photoluminescence (PL) spectra of Cu-Cu<sub>2</sub>O-SiO<sub>2</sub> nanocomposites have been studied at the different % of Cu. The PL spectra of the samples are presented in Fig. 6.5. Additionally, we have also recorded the PL spectrum of our synthesized bare Cu with Cu<sub>2</sub>O NPs, which is shown in Fig. 6.5. It can be seen from figure that the intense photoluminescence band is located mainly at ~ 560 nm (2.21 eV) [49]. The bulk copper is showing the maximum of PL band at 2.11 eV that is somewhat lower on energy than that of the Cu band; which is observed at ~ 560 nm (2.21 eV) in our samples [25]. This small shift can be attributed to the coupling of the incoming and outgoing photons to the plasmon. As per the literature, the relative intensity of characteristic Cu band increases at the decrease of Cu nanoparticle size, i.e. the photoluminescence efficiency increases at the decrease of the size. In other words, the small metal nanoparticles “lighten” better than the bulky ones [26]. Therefore, one can assume that the increase of the efficiency of the photoluminescence of Cu nanoparticles, which is observed in our investigation. Since the photons couple to the surface plasmon, an effect of efficiency increase has to be stronger in the particles where the relative contribution of the surface effects versus volume ones is higher, i.e. in the small particles. Thus, the Cu band in the observed PL spectrum is caused by the recombination of the conduction band electrons with valence band holes, and the increase of the photoluminescence efficiency with the decrease of Cu nanoparticles size is due to the great enhancement of the incoming exciting light and the outgoing emitted light via the coupling of the light to the surface plasmon [25, 26].

In case of supported Cu NPs in SiO<sub>2</sub> matrix, the intensity of characteristic band of Cu NPs goes on decreasing due to less of PL metallic centers; while there is appearance of new band in red region.

We have marked this band for supportive  $\text{SiO}_2$  matrix. This maxima is located at  $\sim 601$  nm with less intense band at 670 nm [26]. At the lowering of the composition from higher to lower, the intensity of these bands decreases drastically, and the single bands of Cu NPs become the dominant in the spectra. The behaviour of the PL spectra described above is evidence that these bands appearing in the spectra at supporting are caused by some centers where the electronic excitations can be localized. Also, due to lesser composition of  $\text{Cu}_2\text{O}$  particles in the composite, there representative PL bands are not observed at 450 nm and 475 nm [26].

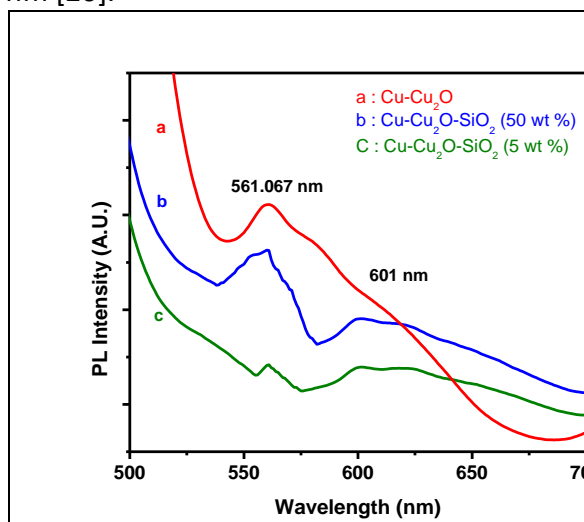


Fig. 6.5: Photoluminescence spectra of Cu-Cu<sub>2</sub>O and Cu-Cu<sub>2</sub>O-SiO<sub>2</sub>.

### 3.3 Optical absorption properties

Fig. 1.4 shows the UV-visible absorption spectra of the Cu-Cu<sub>2</sub>O-SiO<sub>2</sub> nanocomposites in aqueous solution. In all spectra, the surface plasmon resonance (SPR) band is observed at 592 nm for Cu NPs [27]; while the broad absorption edge from 450 to 550 nm is noted for Cu<sub>2</sub>O and SiO<sub>2</sub> particles [28].

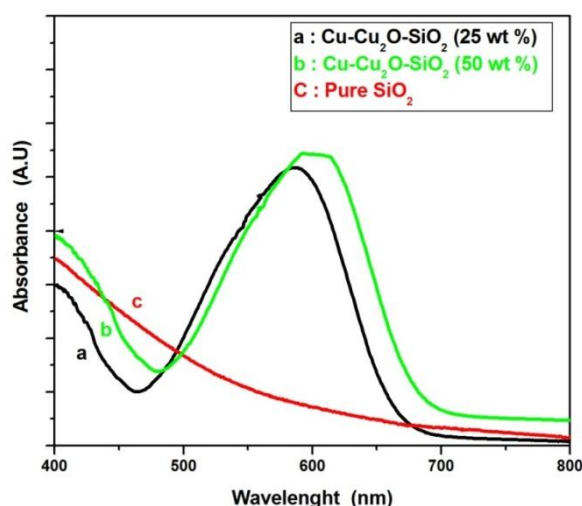


Fig. 1.4: UV-Visible spectra of pure SiO<sub>2</sub> and Cu-Cu<sub>2</sub>O-SiO<sub>2</sub>.

## 4 CATALYTIC STUDIES

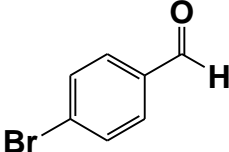
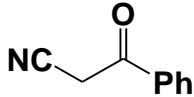
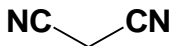
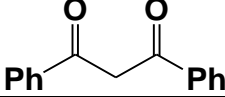
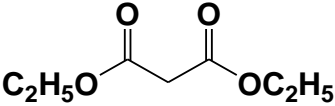
The catalytic activities of Cu-Cu<sub>2</sub>O-SiO<sub>2</sub> nanocomposites have been tested towards the Knoevenagel condensation reaction of 4-Bromobenzaldehyde and different substituted active

methylene compounds in water as a solvent. It is observed that all the reactions occurred rapidly and are completed in 3-5 minutes giving excellent yields of the Knoevenagel products.

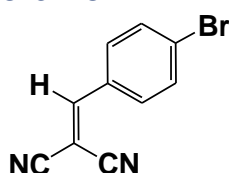
To determine the appropriate composition of the catalysts, we investigated the reaction at different composition of copper nanoparticles such as 5, 25 and 50 wt% supported on SiO<sub>2</sub> matrix. It is noted that 50 wt% copper NPs supported on SiO<sub>2</sub> yields large amount of products than that of other compositions. Therefore, the further catalytic studies are carried out using 50 wt% of Cu-Cu<sub>2</sub>O-SiO<sub>2</sub> nanocomposite. The reactants and products formed with their percentage yield as well as melting point, in this condensation, are summarized in Table 1.1.

The yield of the products was in the range of 82-88 %, which reveals that, Cu-Cu<sub>2</sub>O-SiO<sub>2</sub> (50 wt %) gave better yield with better selectivity also. Active methylene compounds with strong electron withdrawing groups (-CN) giving better yields in short time as compared to that of others.

**Table 1.1: Cu-Cu<sub>2</sub>O-SiO<sub>2</sub> (50 wt %) catalysed Knoevenagel condensation of 4-Bromobenzaldehyde and different substituted active methylene compounds.**

Sr. No.	Aldehyde	Different Active Methylene Compounds	Time (min)	Yield (%)	M.P. (°C) Observed
1			3.5	84	152-154
			3	88	154 – 156
			5	82	166-168
			4	86	150-152

## 5. SPECTRAL DATA OF SELECTED COMPOUNDS



**2-(4-Bromobenzylidene) malononitrile:** Solid; **M.P.:** 154-156°C (Lit<sup>29</sup>. 158°C);

**IR (KBr):** 3099, 2992, 2359, 2224, 1576, 1213, 820, 774, 614cm<sup>-1</sup>;

**<sup>1</sup>H-NMR (CDCl<sub>3</sub>):** δ 7.71 (d, 2H, J = 7.8 Hz), 7.74 (s, 1H), 7.79 (d, 2H, 8.2 Hz).

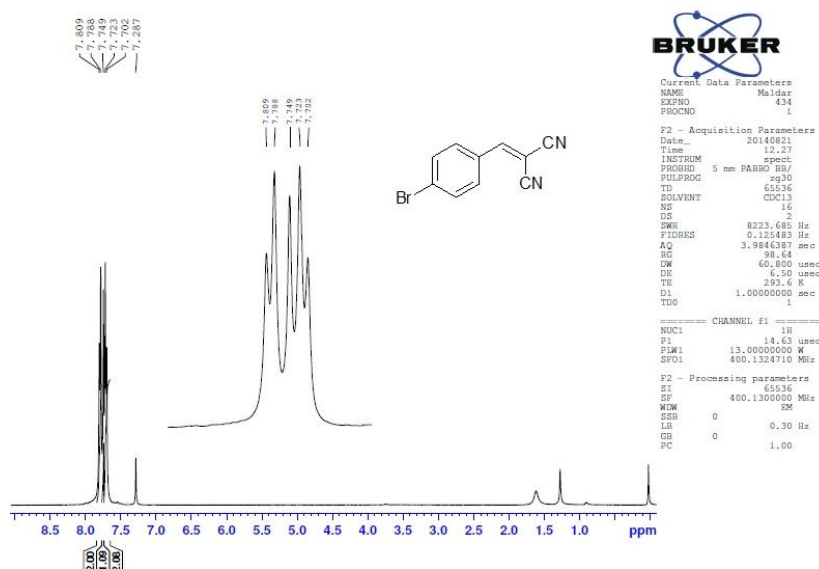


Fig. 1.5:  $^1\text{H}$  Spectra of 2-(4-Bromobenzylidene) malononitrile

## 6. CONCLUSIONS

We have developed an expedient and clean protocol for the synthesis of Knoevenagel condensation products. This method has the advantages of a wide scope of substrates, operational simplicity, easy work-up procedures, shorter reaction times, and high yields.

## REFERENCES

- [1] B. M. Trost and I. Fleming, *Comprehensive Organic Synthesis*, vol. 1–9, Pergamon Press, New York, NY, USA, 1991.
- [2] D. Basavaiah, A. J. Rao, and T. Satyanarayana, "Recent advances in the Baylis—Hillman reaction and applications," *Chemical Reviews*, vol. 103, no. 3, pp. 811–892, 2003.
- [3] D. E. Sammelson and M. J. Kurth, "Carbon-carbon bondforming solid-phase reactions. Part II," *Chemical Reviews*, vol. 101, no. 1, pp. 137–202, 2001.
- [4] R. R. Huddleston and M. J. Krische, "Enones as latent enolates in catalytic processes: catalytic cycloreduction, cycloaddition and cycloisomerization," *Synlett*, no. 1, pp. 12–21, 2003.
- [5] S. E. Gibson and A. Stevenazzi, "The Pauson-Khand reaction: the catalytic age is here!," *Angewandte Chemie International Edition*, vol. 42, no. 16, pp. 1800–1810, 2003.
- [6] M. Moreno-Monas and R. Pleixats, "Formation of carbon-carbon bonds under catalysis by transition-metal nanoparticles," *Accounts of Chemical Research*, vol. 36, no. 8, pp. 638–643, 2003.
- [7] Z. Tang, Z.-H. Yang, X.-H. Chen et al., "A highly efficient organocatalyst for direct aldol reactions of ketones with aldehydes," *Journal of the American Chemical Society*, vol. 127, no. 25, pp. 9285–9289, 2005.
- [8] M. Asiri, "Synthesis and characterization of dyes exemplified by 2-arylidene-1-dicyanomethyleneindane," *Dyes and Pigments*, vol. 42, no. 3, pp. 209–213, 1999.
- [9] R. Ballini and G. J. Bosica, "Nitroaldol reaction in aqueous media: an important improvement of the Henry reaction," *The Journal of Organic Chemistry*, vol. 62, no. 2, pp. 425–427, 1997.
- [10] Y. Chi and S. H. Gellman, "Diphenylprolinol methyl ether: a highly enantioselective catalyst for Michael addition of aldehydes to simple enones," *Organic Letters*, vol. 7, no. 19, pp. 4253–4256, 2005.

- [11] H. Hattori, "Heterogeneous basic catalysis," *Chemical Reviews*, vol. 95, no. 3, pp. 537–558, 1995.
- [12] F. Figueras, M. L. Kantam, and B. M. Choudary, "Solid base catalysts in organic synthesis," *Current Organic Chemistry*, vol. 10, no. 13, pp. 1627–1637, 2006.
- [13] S. Canning, S. D. Jackson, E. McLeod, and E. M. Vass, "Aldol condensation of acetone over CsOH/SiO<sub>2</sub>: a mechanistic insight using isotopic labelling," *Applied Catalysis A*, vol. 289, no. 1, pp. 59–65, 2005.
- [14] F. Winter, A. J. van Dillen, and K. P. de Jong, "Supported hydrotalcites as highly active solid base catalysts," *Chemical Communications*, no. 31, pp. 3977–3979, 2005.
- [15] R. Garro, M. T. Navarro, J. Primo, and A. Corma, "Lewis acid-containing mesoporous molecular sieves as solid efficient catalysts for solvent-free Mukaiyama-type aldol condensation," *Journal of Catalysis*, vol. 233, no. 2, pp. 342–350, 2005.
- [16] Smahi, A. Solhy, H. El Badaoui et al., "Potassium fluoride doped fluorapatite and hydroxyapatite as new catalysts in organic synthesis," *Applied Catalysis A*, vol. 250, no. 1, pp. 151–159, 2003.
- [17] S. Wada and H. Suzuki, "Calcite and fluorite as catalyst for the Knövenagel condensation of malononitrile and methyl cyanoacetate under solvent-free conditions," *Tetrahedron Letters*, vol. 44, no. 2, pp. 399–401, 2003.
- [18] M. L. Kantam, B. M. Choudary, C. V. Reddy, K. K. Rao, and F. Figueras, "Aldol and Knoevenagel condensations catalysed by modified Mg-Al hydrotalcite: a solid base as catalyst useful in synthetic organic chemistry," *Chemical Communications*, no. 9, pp. 1033–1034, 1998.
- [19] K. Akutu, H. Kabashima, T. Seki, and H. Hattori, "Nitroaldol reaction over solid base catalysts," *Applied Catalysis A*, vol. 247, no. 1, pp. 65–74, 2003.
- [20] B. M. Choudary, M. L. Kantam, C. V. Reddy, K. Koteswara Rao, and F. Figueras, "Henry reactions catalysed by modified Mg-Al hydrotalcite: an efficient reusable solid base for selective synthesis of  $\beta\beta$ -nitroalkanols," *Green Chemistry*, vol. 1, no. 4, pp. 187–189, 1999.
- [21] K. A. Utting and D. J. Macquarrie, "Silica-supported imines as mild, efficient base catalysts," *New Journal of Chemistry*, vol. 24, no. 8, pp. 591–595, 2000.
- [22] S. M. Lai, C. P. Ng, R. Martin-Arnade, and K. L. Yeung, "Knoevenagel condensation reaction in zeolite membrane micro-reactor," *Microporous and Mesoporous Materials*, vol. 66, no. 2-3, pp. 239–252, 2003.
- [23] O.H. Abd-Elkader, N.M. Deraz, *International Journal of Electrochemical Science*, vol.8, pp.8614,2013.
- [24] R. Ullah, B. K. Deb, M.Y. Ali Mollah, *International Journal of Composite Materials*, vol. 4 pp. 135, 2014.
- [25] Mooradian, *Physical Review Letters*, 22 (1969) 185.
- [26] O.A. Yeshchenko, I. M. Dmitruk, A. M. Dmytruk, A. A. Alexeenko, *Materials Science and Engineering B*, 137 (2007) 247.
- [27] K. Tian, C. Liu, H. Yang, X. Ren, *Colloids and Surfaces A*, vol. 397, pp.12, 2012.
- [28] H.R. Nikabadi, N. Shahtahmasebi, M. Rezaee Rokn-Abadi, M.M. Bagheri Mohagheghi, E.K. Goharshadi, *Physica Scripta*. vol.87, pp. 25802, 2013.
- [29] M.B. Deshmukh, S.S. Patil, S.D. Jadhav, P.B. Pawar, *Synthetic Communications*, vol.42, pp.1177, 2012.